*Manuscript
Click here to download Manuscript: R3.HYDROL11970.doc
Click here to view linked References

Evaluation of evaporation estimation methods for a covered reservoir in a semi-arid climate (south-eastern Spain)

B. Gallego-Elvira, A. Baille, B. Martín-Gorriz, J.F. Maestre-Valero and V. Martínez-Alvarez*

Technical University of Cartagena. Agricultural Engineering Section. Paseo Alfonso XIII, 48. 30203 Cartagena (Spain).
**Correspondence to: Victoriano Martínez-Alvarez. Technical University of Cartagena. Agricultural Engineering Section. Paseo Alfonso XIII, 48. 30203 Cartagena (Spain).*
E-mail: victoriano.martínez@upct.es

Abstract

The main purpose of this study was to evaluate different methods of evaporation estimation for covered water reservoirs. A reservoir equipped with a suspended cover was fully monitored to register the evaporation rate and microclimate below the cover. The datasets were used to evaluate the performance of commonly used evaporation methods, namely energy budget, mass-transfer, combination (Penman and FAO-56 Penman-Monteith) and floating class-A pan. The mass-transfer formula based on the Sherwood number proposed for free convection conditions, which were observed to prevail below the cover, supplied reasonably good estimates of covered reservoir evaporation and it is a good option from a practical point of view, with low input data requirements. Detailed input data and modifications in the calculation of energy fluxes are required to get good evaporation estimations of covered surfaces with the energy budget and FAO-56 Penman-Monteith methods. Besides, some of the standard meteorological input data (such as wind speed at 2m height) cannot be registered below the cover. Penman equation presented a poor performance related to the overestimation of the advective component for free convection conditions. The pan evaporation was found to be substantially higher than the reservoir evaporation, due to the particular characteristics of the tank, that increased surface temperature and hence evaporation rate. A simplified empirical mass-transfer formula was also proposed to estimate evaporation of covered water bodies from the only knowledge of the surface-to-air mixing ratio gradient.

Key words: Shade covers; water storages; water losses; Sherwood number; free convection; floating class-A pan.

1. Introduction

Identification and control of water losses other than crop consumptive use are important issues in irrigation water management. Evaporation from water storages is undesirable and unrecoverable (Carter et al., 1999), representing an important fraction of the stored water, particularly in arid and semiarid climates (Gokbulak and Ozhan, 2006; Martínez-Alvarez et al., 2008; Mugabe et al., 2003). Several methods have been proposed to prevent evaporation, such as floating materials (Daigo and Phaovattana, 1999), chemical products (Barnes, 2008), wind shelters (Hipsey and Sivapalan, 2003) or suspended shade nets (Craig et al., 2005; Martínez-Alvarez et al., 2010). Suspended shade covers have been pointed out as one of the most promising techniques for mitigating evaporation losses. It was demonstrated that the presence of an opaque porous black polyethylene cover induced strong microclimate changes near the water surface with respect to an uncovered surface, leading to evaporation loss reduction up to 85% (Gallego-Elvira et al., 2011). To assess the performance of different types of cover material, a simplified and reliable method for estimating evaporation loss of covered reservoirs from climate data would be especially useful.

Direct measurement of the evaporation rate from a covered reservoir might be performed by monitoring the water level with pressure transducers as in open-water conditions. However, the overall precision would be rather low because the daily evaporation rate is generally lower than 1 mm day^{-1} while the accuracy of the pressure transducers currently available is of the order of ±0.5mm. A more precise measuring method would be to place a floating evaporation pan provided with an accurate level-meter (accuracy: ±0.10mm), assuming that the pan evaporation is representative of the reservoir evaporation. The main advantage of the floating pan is that evaporation measurements are independent of changes in reservoir level due to outflows (e.g. irrigation, seepage) or inflows (refilling), which is the case of most operating water storages. Floating class-A pans have been used to estimate evaporation of open-water reservoirs since they simulate the physical conditions on the water surface that control evaporation (Masoner et al., 2008). However, under covered conditions, the assumption that the evaporation rate of the reservoir is close to that of the floating pan is not ascertained. The differences in boundary conditions and thermal stratification are likely to induce different water surface temperature, hence different evaporation rate from the two water bodies.

Several methods are currently used to predict evaporation from meteorological data for open-water reservoirs. They are generally categorized into: temperature and radiation (Xu and Singh, 2000, 2001), mass-transfer (aerodynamic) (Singh and Xu, 1997), pan coefficient (Fu et al., 2004), energy budget and combination methods (Gianniou and Antonopoulos, 2007; Rosenberry et al., 2007). These methods have been validated and calibrated for open-water surfaces, but to our knowledge, the parameterisation and validation of the above-mentioned methods for covered reservoirs have not yet been undertaken. The energy budget and combination methods have been reported to provide reliable and robust evaporation predictions (Ali et al., 2008; Delclaux et al., 2007; Rosenberry et al., 2007) but are not the most appropriate as routine methods, due to the high data requirements for estimating the net radiation (R_n) and conduction heat flux (G). Moreover, R_n and G can be of the same order of magnitude for cover conditions (Gallego-Elvira et al., 2011), likely leading to large relative errors in the estimation of the available energy component, $R_n – G$. A more suitable option, less demanding in terms of input data, is to use the mass-transfer method, although it requires to identify the mass-transfer coefficient (or 'wind' function) and how the latter is related to the microclimate variables prevailing under the cover. The added problem is that 'wind' functions obtained for open reservoirs assuming forced convection, are probably not valid under covered reservoirs, where very low wind speed and large surface to air temperature gradients prevail (Martínez-Alvarez et al., 2010), creating free or mixed convection regime conditions. Note that these specific conditions also invalidate the use of the wind function that is included in commonly used Penman formula to estimate the advective component.

To determine evaporation in a free convective state, equations including the Sherwood number (*Sh*) for evaporation have been proposed (Jacobs and Verhoef, 1997). For these conditions, *Sh* can be determined from a relation with the Rayleigh number (*Ra*) (Pauken, 1998; Bower and Saylor, 2009). Most of the studies dealing with evaporation under free or mixed convection state are focused on the situation when water surface temperature is higher than ambient air (Bower and Saylor, 2009). This is commonly the case of open-water bodies, wet soils or heated pools for different purposes (Pauken, 1999). However, for indoor conditions like greenhouses with freely transpiring crops or water bodies covered with shading nets, the vegetated or water surface might be at lower temperature than the air. In that case, a stable profile (thermal stratification) is established, damping the turbulent free convective flow and reducing the intensity of heat and mass transfer between the water surface and the surrounding air.

The main objective of the present study is to evaluate different methods for estimating evaporation from covered water reservoirs. The performance of the methods: energy budget, mass-transfer, combination (Penman and FAO-56 Penman-Monteith) and floating class-A pan, has been tested against a detailed experimental dataset that provided all the input variables required for the comparative study. The suitability and practical applicability of each method is discussed. Particular focus has been given to the mass-transfer formula based on the Sherwood number proposed for free convection, since these conditions were observed to prevail below the cover. Besides, a mass-transfer formula has been empirically derived to predict evaporation of the covered reservoir.

2. Materials and methods

2.1. Reservoir and cover description

Evaporation (E) and microclimate measurements were collected for an experimental irrigation reservoir equipped with a suspended cover located at the Experimental Station of the University of Cartagena in south-eastern Spain (37º35'N, 0º59'W). The data collection period was from 12th June to 27th August 2009. The reservoir has a surface of 2,500 m^2 and 5 m depth and it is waterproof by means of a plastic liner.

The shade cover consists on a porous cloth suspended above the water surface by means of a high tension polyamide cable structure. The shade cloth is a double layer mesh made of black polyethylene (ATARFIL S.L., ATARSUN shade cover). The cable framework has wires under the cloth to hold the mesh and above to prevent wind suction. This cover achieved a reduction of 85% in the annual evaporation loss (Martínez-Alvarez et al., 2010). The cover was also reported to effectively shelter the water surface from wind (92% reduction) and solar radiation (99% reduction).

Reference weekly evaporation reduction factors achieved by the cover during the experimental period are presented in Table 1. FAO-56 Penman-Monteith reference evapotranspiration values (ET_o, Allen et al., 1998) were used as estimates of open-water evaporation (Craig, 2006). ET_o values were provided by the station CA12 of the agro-meteorological network SIAM (Servicio de Información Agraria de Murcia, http://siam.imida.es), which is located 100m from the experimental reservoir. The reduction factors (RF, %) were computed as $(ET_o-E)/ET_o$.

Table 1. Reference weekly evaporation reduction factors achieved by the cover during the 11-week experimental period

2.2. Evaporation and microclimate measurements

The water level of the reservoir was monitored with a pressure sensitive transducer immersed in the water body (Druck, PDCR1830, accuracy: ±0.45mm). A floating class-A pan equipped with an accurate water level sensor (Temposonics, MTS sensor C-series, accuracy: ±0.10mm) was deployed in the covered reservoir (Fig. 1). The floats of the pan were dimensioned to make the water surface of the pan and reservoir being on the same level.

The meteorological evaporation-driving variables of the air between the cover and water surface (inner air) were continuously surveyed during the experimental period. The climate sensors were implemented on a metallic structure attached to a raft in order to register the microclimate data at 0.3m above the water surface (Fig. 1). The following variables were measured: air temperature, T_a, and relative humidity, RH, (Vaisala, HMP45C probe) and wind speed, U, (UPCT, BLC-Y low wind speed sensor). Eleven temperature probes (Campbell, T-107) provided the temperature profile of the covered reservoir. They were placed at the following depths: surface (T_s), 0.33m, 0.66m, 1m, 1.5m, 2m, 2.5m, 3m, 3.5m, 4m and 4.5m. A temperature probe (Campbell, T-107) was also installed in the floating pan to measure the temperature of the water surface, $T_{s,p}$. The temperature of the cover, T_C, was measured by means of an infrared temperature sensor (Apogee, IRR-S). All sensors were scanned at 10s intervals and hourly average values were recorded by means of two dataloggers (Campbell, CR1000). The hourly data were processed to obtain the daily mean values of the variables.

Fig 1. Data collection layout in the covered reservoir (the vertical scale is exaggerated for clarity)

2.3. Weekly values of evaporation

Daily evaporation values for the reservoir (E) and the floating class-A pan (E_{pan}) were directly derived from water level measurements and then weekly averaged. The weekly scale was selected for assessing the performance of the evaporation methods since the accuracy of the water level sensor of the reservoir was limited to ±0.45mm.

Estimations of the evaporation rate were first calculated on daily scale from the hourly meteorological data with all methods and then averaged to weekly scale to be compared with evaporation measurements.

3. Evaporation methods

3.1. Energy budget for covered conditions

The energy balance at the surface of a water body can be expressed as the balance of energy gains and losses as follows:

$$R_n + \lambda E_{EB} + G + H = 0 \quad (1)$$

where R_n is the net radiation at the water surface, λE_{EB} is the latent heat flux, G the heat flux into the underlying water body and H the sensible heat exchanged between the air and the water surface. The sign convection is that both fluxes G and H are considered positive when directed towards the surface (and therefore represent energy available for evaporation), and negative when leaving the surface. G can be considered equal to the heat storage rate by assuming that the contribution of the other terms affecting energy storage (heat transfer to substrate and retaining materials, inflows, outflows…) is small and negligible (Gianniou and Antonopoulos, 2007; Rosenberry et al., 2007). All fluxes are expressed in W m^{-2}, if not mentioned otherwise.

For a covered reservoir the net radiation at the water surface can be expressed as (Gallego-Elvira et al., 2011):

$$R_{n,C} = (1-a)\ S_t + (1-b)(L_{a,t} + L_C) - L_w \quad (2)$$

where $R_{n,C}$ is the net radiation at the covered water surface, S_t and $L_{a,t}$ are the solar and atmospheric radiation transmitted by the cover, respectively, L_C and L_w are the long-wave radiation emitted by the cover and the water surface, respectively, and a and b are the albedo and long-wave reflectivity of the water surface. L_w and L_C can be calculated from surface temperature by means of the Stefan-Boltzmann equation (water emissivity = 0.97, black polyethylene cover emissivity ≈ 1).

To determine the heat storage in a covered reservoir, thermal stratification has to be considered (Gallego-Elvira et al., 2011). G can be estimated by dividing the water body into layers (l) corresponding to each temperature sensor available with the following expression:

$$G = C_w \sum_{j=1}^{j=l} z_j \frac{\Delta T_{wj}}{\Delta t} \quad (3)$$

where C_w (J m^{-3} ºC^{-1}) is the volumetric heat capacity of water at the temperature of each layer, z_j (m) stands for the depth of each layer (in this study: 0.33m in the first meter and 0.5m for the rest, l=11, $T_{w1}=T_s$) and ΔT_{wj} (ºC) is the change in water temperature of each layer during a time step.

The sensible heat exchange at the reservoir air–water interface can be calculated as:

$$H = h_c (T_a - T_s) \quad (4)$$

where T_a and T_s (ºC) are the air and water surface temperature, respectively, and h_c (W m^{-2} K^{-1}) is the coefficient of convective heat exchange.

For free convection conditions h_c can be computed from the Nusselt number (Nu) as follows (Incropera and DeWitt, 1996):

$$h_c = \frac{Nuk}{L} \quad (5)$$

where L (m) is the characteristic length and k (W m^{-1} K^{-1}) is the heat conductivity of air.

Once $R_{n,C}$, H and G are computed, the evaporation rate (E_{EB}) is calculated as a residual of Eq. 1, forcing the closure of the energy balance.

3.2. Mass-transfer

3.2.1. Forced convection

The mass-transfer method, based on Dalton's law, assumes that evaporation is driven by the vapour pressure gradient between the water surface and the surrounding air, and modulated by the nearby environment through a mass-transfer coefficient, usually considered as linearly dependent on wind speed and termed 'wind' function. The general expression of the mass-transfer formula for a freely evaporating water surface is:

$$E = f(U)\,(e_s - e_a) \tag{6}$$

where e_s is the saturation vapour pressure at the temperature of the water surface, e_a is the vapour pressure of the ambient air and $f(U)$ is the wind function. A good review of proposed wind functions can be found in Singh and Xu (1997).

Mass-transfer formulae empirically derived for open-water bodies exposed to wind are not suitable for covered surfaces highly protected from wind. A mass-transfer formula which only depends on surface-to-air mixing ratio gradient (X_s - X_a) is proposed in this study for covered water surfaces (Eq. 14). The mass-transfer coefficient was empirically deduced from evaporation measurements of the covered reservoir ($h_{m,C}$, mm day^{-1} g^{-1} kg) and the floating pan ($h_{m,p}$, mm day^{-1} g^{-1} kg) with the following equation:

$$h_{m,C} = \frac{E}{(X_s - X_a)} \tag{7}$$

where E is the measured evaporation rate (mm day^{-1}) in the covered reservoir and X_a and X_s are the water vapour mixing ratio of air and water surface (g water (kg air)$^{-1}$), respectively. Values of evaporation and water vapour mixing ratio of the floating pan were taken to calculate $h_{m,p}$ with Eq. 7.

3.2.2. Mass-transfer formulae for free or mixed convection based on Sherwood number

Under free or mixed convection regimes, which prevail in covered conditions, the evaporation rate can be determined from the knowledge of the Sherwood number (Sh), the temperature and humidity of surrounding air and water surface temperature, using the following mass-transfer formulae (Jacobs and Verhoef, 1997):

$$E_{Sh} = \frac{Sh\ D\ \rho\ (X_s - X_a)}{L} \tag{8}$$

where E_{Sh} is the evaporation rate (g m^{-2} s^{-1}), D is the molecular diffusion coefficient of water vapour in air (m^2 s^{-1}), ρ is the air density (kg m^{-3}) and L (m) is the characteristic length (L = 45m for reservoir and L = 1.2m the floating pan). Sherwood number is defined as follows:

$$Sh = \frac{h_m \ L}{D} \tag{9}$$

Sh represents the ratio of the convective mass-transfer coefficient (h_m, m s^{-1}) to the diffuse mass-transfer coefficient, D. Assuming analogy between heat and mass transfer, *Sh* can be derived from the Nusselt number (Appendix).

To determine whether the type of convection is free, forced or mixed, criteria based on the ratio of buoyancy to inertial forces (= Ra/Re^2, where *Ra* is the Rayleigh number (Eq. A.3) and *Re* is Reynolds number = $U\,L/\nu$, with U being the air velocity near the surface and ν the kinematic viscosity) are generally used (Jacobs and Verhoef, 1997):

$$\begin{array}{ll} Ra < 0.1Re^2 & \text{forced convection} \\ 0.1Re^2 < Ra < 16Re^2 & \text{mixed convection} \\ Ra > 16Re^2 & \text{free convection} \end{array} \tag{10}$$

3.3. Combination

Combination methods derive evaporation by combining radiation and aerodynamic energies into one equation.

3.3.1. Penman formulae

In the last 60 years, one of the most commonly used formulae to derive open-water evaporation from meteorological data has been the Penman equation (Penman, 1948). It is a physically based expression that combines the mass-transfer and energy budget approaches. The classical form for the Penman equation is (Valiantzas, 2006):

$$E_P = E_{Pr} + E_{Pa} = \left(\frac{\Delta}{\Delta+\gamma}\right)\frac{R_n}{\lambda} + \left(\frac{\gamma}{\Delta+\gamma}\right)\frac{6.43(1+0.54U)(e_a^* - e_a)}{\lambda} \tag{11}$$

where E_{Pr} is usually referred to as the *equilibrium* evaporation or radiative component and E_{Pa} is generally named the *advective*, or aerodynamic component (Brutsaert, 1982). Δ is the slope of the saturation vapour pressure curve (kPa °C^{-1}), γ is the psychometric constant (kPa °C^{-1}), λ is latent heat of vaporization (MJ kg^{-1}), e_a^* (kPa) is the saturation vapour pressure of the air and R_n is commonly calculated with the FAO-98 approach which does not require water temperature data. Eq. 11 does not allow for heat storage and therefore it would be only suitable for very shallow water bodies. In order to improve the accuracy of the estimations the heat storage should be considered, and when water temperature is known the term R_n should be substituted for R_n-G.

To adapt this equation to covered conditions, R_n can be calculated with Eq. 2 and G with Eq. 3 to compute the radiative component. However, the advective component includes a wind function derived for open-water conditions not suitable for covered water surfaces. The accuracy of evaporation predictions for covered conditions has been tested with the original wind function to assess the errors derived from its use.

3.3.2. FAO-56 Penman-Monteith

The Penman Monteith FAO56 (PM-FAO56) equation is the standard method to predict daily reference evapotranspiration (ET_o, Allen et al., 1998) and it has been reported to give a good estimation of reservoir open-water evaporation (Craig, 2006). The PM-FAO56 equation may be written as:

$$E_{PM} = E_{PMr} + E_{PMa} = \frac{0.408\Delta(R_n - G)}{\Delta + \gamma(1 + 0.34U)} + \frac{\gamma(900/(T_a + 273))U(e_a^* - e_a)}{\Delta + \gamma(1 + 0.34U)} \qquad (12)$$

where E_{PMr} and E_{PMa} are the radiative and the advective components. As in the case of Penman, R_n was calculated with Eq. 2 and G with Eq. 3, to adapt these terms to covered conditions. For standard determination of PM-FAO56 ET_o, the input meteorological data should be measured at 2m above the surface. Note that in this study the meteorological variables are measured at 0.3m above the water surface from a floating station.

4. Results and discussion

4.1. Microclimate conditions below the cover

4.1.1. Temperature gradients

Fig. 2 presents the daily evolution of following temperatures: cover, inner air, water surface of the reservoir and of the floating pan. The data of the floating pan has been included to show the difference in water surface temperature with the reservoir, which is directly related with the difference in the surface-to-air mixing ratio gradient (Fig. 3) and therefore with the evaporation rate. During the whole experimental period a stable temperature profile was observed. The daily average temperature of the cover was above the inner air temperature and the latter was above the water surface temperature of both reservoir and floating pan. The cover reached very high temperatures (up to 57ºC, hourly average registered at noon) due to its high absorption of solar radiation and heated the inner air which surpassed 49ºC in summer afternoons. The inner air was on daily average for the study period 6.5ºC (±1.1ºC) above the reservoir water surface temperature and 3.8ºC (±0.8ºC) over the floating pan water surface temperature. The latter values indicated strong thermal stratification and prevalence of buoyancy-driven heat exchange mechanisms that transfer heat from the inner air down to the water surface, therefore supplying energy for the evaporation process.

Fig. 2. Daily evolution of temperature of the cover (T_C), inner air (T_a) and water surface of the floating pan ($T_{s,p}$) and of the reservoir (T_s), during the 11-week experimental period

4.1.2. Wind speed

Very low wind speeds were observed below the cover. On daily average, the wind speed measured 0.3m above water surface varied from 0.18 to 0.32m s^{-1} (study period average: 0.24±0.02m s^{-1}). This is the consequence of the shelter provided by the cover against outside wind whose speed varied from 1.42 to 5.24m s^{-1} (study period average: 2.06±0.62m s^{-1}).

4.1.3. Water vapour mixing ratio

The vapour mixing ratio gradient is the main driving-force of evaporation, i.e. it is the gradient that determines the mass transfer between the water surface and the surrounding air. The vapour mixing ratio of the inner air (X_a) remained on average 2.26 (±1.05)g water (kg air)$^{-1}$ below the vapour mixing ratio of the reservoir water surface (X_s). The average vapour mixing ratio gradient between pan water surface ($X_{s,p}$) and inner air was 5.73 (±1.23)g water (kg air)$^{-1}$ (Fig. 3). The higher gradient of the pan ($X_{s,p}$ - X_a) compared to the reservoir (X_s - X_a) is ascribed to the difference between water surface temperature of the pan and the reservoir (Fig. 2), which meant that the saturation vapour pressure at the temperature of the water surface for the pan was on average 0.56 (±0.15)kPa above the saturation vapour pressure for reservoir surface. This led to higher evaporation rates in the pan and therefore the evaporation measured in the pan overestimates the actual evaporation of the reservoir (Fig. 5).

Fig 3. Daily evolution of water vapour mixing ratio of the floating class-A pan ($X_{s,p}$), of the reservoir (X_s) and of the inner air (X_a), during the 11-week experimental period

4.1.4. Assessment of the convection regime

To assess the type of convection regime prevailing below the cover, the criteria of Eq.10 were considered. Table 2 summarizes the values of *Ra*, Re^2 and Ra/Re^2 that allowed the assessment of the convection regime.

Table 2. Values of *Ra*, Re^2 and Ra/Re^2 to determine the type of convection

The high temperature gradient between water surface and inner air and the low wind below the cover meant relatively high *Ra* and low *Re* values, characteristic of free convection. The reservoir clearly presented free convection conditions according to the criteria $Ra > 16Re^2$ and mixed convection regime ($0.1Re^2 < Ra < 16Re^2$) prevailed for the floating class-A pan.

4.2. Energy balance at the covered surface

Covered surfaces present important modifications on the magnitude, sign and relative weight of the components of the energy balance, which have been observed to be reduced up to one order of magnitude compared to uncovered conditions (Gallego-Elvira et al., 2011). The major fluxes in the energy balance of the covered surface are the incoming (L_C = 482±8.72W m^{-2}) and outgoing (L_w = 435±5.37W m^{-2}) long-wave radiation at the water surface. The reflected long-wave radiation only accounted for 14.41±0.25W m^{-2} and the transmitted (short- and long-wave) radiation by the cover can be neglected since the reservoir was covered with an opaque black polyethylene cloth (Martínez-Alvarez et al., 2010). Although the low evaporation flux is close to $R_{n,C}$ (Fig. 4), the other fluxes, especially heat storage, should be accounted for because they have the same order of magnitude as λE. The sensible heat flux represents a small energy input to the surface since the water surface is on daily scale always colder than the inner air. The water layers were slowly heating up during the experimental period, and therefore these weeks the term G had a negative sign, since this energy was not available at the water surface for evaporation. Note that, the heat storage can represent an important energy input to the water surface (i.e. enhancing evaporation), of even higher magnitude than $R_{n,C}$, when all the heat stored during heating period is released after the overturn of the water profile (Gallego-Elvira et al., 2011).

The weekly averages of the daily energy balance terms at the covered water surface are depicted in Fig. 4. $R_{n,C}$, G and H were computed from measurements with Eqs. 2, 3 and 4, respectively, and λE corresponds to the evaporation flux derived from water level measurements. Looking into the energy balance closure, it was observed that the sum of sensible and latent heat fluxes ($H + \lambda E$) was lower than the difference between net radiation and heat storage (available energy: $A = R_{n,C} + G$). The average 11-week period energy balance residual ($r = H + \lambda E + R_{n,C} + G$) was 7.08±4.66W m^{-2}, which corresponds to 26.26±14.83% of A. The absolute residual is observed to be reduced one order of magnitude, compared to the common residuals observed in open surfaces (Foken, 2008).

Fig. 4. Weekly evolution of the energy fluxes at the covered water surface. Experimental period: 12th June to 27th August 2009.

4.3. Suitability of floating class-A pan evaporation measurements for covered reservoirs

Although floating class-A pans have been reported to provide a good estimation of open-water evaporation, the results of this study show that for covered conditions the pan substantially overestimates the reservoir evaporation, even though the surrounding atmospheric conditions were the same. The pan presented markedly higher daily water surface temperature (average difference with the reservoir: 2.72±0.59ºC, Fig. 2), which led to higher vapour-mixing-ratio gradient (i.e. higher evaporation driving gradient, Fig. 3). This meant that the evaporation in the floating pan was markedly higher (MBE = 0.44 mm day^{-1}, Table 3) than the reservoir evaporation and therefore, for estimating covered evaporation from pan measurements, a pan coefficient ($=E/E_{pan}$) would be required. The average pan coefficient observed in this trial was 0.63 (±0.07). This value can not be used for further calculations since the length of this trial was only 11 weeks and important seasonal variation of this coefficient has been observed (Martínez-Alvarez et al., 2007). Besides, this value can vary depending on the operating conditions of the reservoir (inflows temperature and frequency). Further data collection would be necessary to characterise the annual evolution of this coefficient and how the different operating conditions scenarios would affect its value.

4.4. Performance of the evaporation estimation methods

The accuracy and suitability of the evaporation methods above-described have been tested for covered conditions. To assess the accuracy of the methods, the statistical estimators (computed as in Crawford and Duchon, 1998): root mean squared error (RMSE), mean bias error (MBE) and maximum absolute error (MaxAE) are provided in Table 3 with the mean and standard deviation (SD) of weekly averages of daily evaporation measurements and estimations. Fig. 5 shows the weekly average values of observed and calculated daily evaporation in order to give an overview of the methods performance. The suitability of each method for covered surfaces is discussed in the next subsections.

The MBE, which quantifies systematic errors, indicated that the Penman equation values systematically overestimated the evaporation in the covered reservoir. The Energy Budget (EB) and PM-FAO56 methods slightly overestimated evaporation while the Sherwood formula did not produce any substantial systematic error, outperforming the other methods. The RMSE, which measures both systematic and non- systematic errors, was also the lowest when using the Sherwood method (RMSE = 0.08mm day^{-1}), followed by the PM-FAO56 and EB methods (RMSE = 0.22mm day^{-1} and 0.30mm day^{-1}, respectively). The Penman equation produced markedly higher errors than the rest, highlighting that this method is not suitable for covered surfaces. These results indicate that good estimates of evaporation loss from covered water reservoirs can be obtained from Sherwood number method, which had been proposed for free convection conditions, and also reasonable good estimates can be provided by the PM-

FAO56 and EB methods considering the indicated modifications (Eqs. 2 and 3) in the calculation of the energy fluxes at the covered water surface.

Table 3. Mean values and Standard Deviation of weekly averages of daily evaporation measurements and estimations for the 11-week experimental period. Statistical estimators for estimations of covered reservoir evaporation

Fig. 5. Comparison of weekly averages of daily values of measurements of covered reservoir evaporation (E) with floating class-A pan measurements (E_{pan}) and estimations calculated by Sherwood (E_{Sh}), Energy Budget (E_{EB}), Penman (E_P) and PM-FAO56 (E_{PM}) methods. Experimental period: 12th June to 27th August 2009.

4.4.1. Sherwood method

Equations to predict evaporation based on Sherwood number had been proposed for free or mixed convection state on the situation when water surface temperature is higher than ambient air (Bower and Saylor, 2009). In this study, the performance assessment shows that this method provides good estimates of evaporation for covered water surfaces, which normally have lower temperature than the air. Considering its good performance and the low requirements of input data, we point out this method as the most suitable for covered surfaces. To apply this method, it is necessary to install below the cover a temperature and humidity probe and a water surface temperature sensor.

4.4.2. Energy budget

The EB method is considered as the most accurate method to estimate open-water evaporation if the components are evaluated correctly (Rosenberry et al., 2007). This method provided reasonably good estimates of evaporation of the covered reservoir, but according to our results, it did not present better accuracy than the Sherwood method. Since energy fluxes for the covered surface can be reduced up to one order of magnitude with respect to uncovered conditions, errors in the estimation of energy balance terms are relatively more important. The EB method requires more detailed data than Sherwood method such as cover temperature and emissivity to derive the incoming long-wave radiation at the water surface (i.e. radiation emitted by the cover). An error of ±1ºC in the range of observed cover temperatures (12.29 – 57.02ºC, minimum – maximum values registered in the experimental period) can produce errors from 5.23 to 8.12W m^{-2} in the estimation of cover long-wave radiation and an error of ±0.01 in the estimation of cover emissivity can lead to errors from 3.74 to 7.15W m^{-2}. Considering the lower magnitude of the covered-surface net radiation ($R_{n,C}$, 33.10±9.02W m^{-2}, average of study period daily values), these errors could have an important impact on the accuracy of the EB method. Therefore, taking into account the limitations to accurately compute the energy fluxes at the covered water surface and since the simpler Sherwood method can provide good evaporation estimations for these particular conditions, it seems to be a better option for practical applications.

4.4.3. Penman and FAO-56 Penman-Monteith equations

The Penman equation presented substantial overestimation of covered evaporation, whereas the PM-FAO56 method presented a good performance. The radiative component of Penman and PM-FAO56 methods, E_{Pr} and E_{PMr} respectively, which had as input value the available energy flux ($R_{n,C}$ + G), had practically the same value (Fig. 6) and showed a similar pattern to the EB estimations (R^2=0.97 for E_{Pr} vs. E_{EB} and E_{PMr} vs. E_{EB}), although they were about 35% lower. The difference between E_P and E_{PM} is due to advective component. The average calculated value of the advective terms E_{Pa} and E_{PMa}, taking as input wind speed the values registered below the cover (0.24±0.02m s^{-1}), were 1.13±0.07 and 0.26±0.02mm day^{-1}, respectively (Fig. 6). The value of the advective term of Penman equation for a hypothetical situation of wind speed = 0m s^{-1} would be 1.01±0.06mm day^{-1} (E_{Pa0}, Fig. 6), which is higher than the actual evaporation rate in the covered reservoir. The latter highlights that the wind function of the Penman advective term is not suitable for covered conditions and leads to important overestimation. The PM-FAO56 advective term for the rather calm conditions below the cover is very low and do not lead to substantial overestimation (note that for U = 0m s^{-1}, E_{PMa}=0). In fact, the method presented a similar performance to the EB method (Table 3). Since PM-FAO56 and EB methods had the same data requirements and the above-commented accuracy limitations on the energy fluxes determination would also affect the PM-FAO56 estimations, Sherwood method is also recommended over this method from a practical point of view.

Fig. 6. Evolution of weekly averages of daily values of: the radiative and advective terms of the combination methods (Penman (E_P) and PM-FAO56 (E_{PM})), measurements of covered reservoir evaporation (E) and estimations calculated by the Energy Budget method (E_{EB}). The subindex “a” refers to advective, “r” to radiative, and “0” indicates that wind speed was set to zero for calculations. Experimental period: 12th June to 27th August 2009.

4.5. Mass-transfer formula for covered conditions

The mass-transfer coefficient for open-water conditions is normally derived as linearly dependent on wind speed, but for covered conditions since the wind is no longer a major evaporation-driving factor, a mass-transfer formula only dependent on surface-to-air mixing ratio gradient can be proposed to predict evaporation. Pooling the weekly derived values of the mass-transfer coefficients (Eq. 7) for the reservoir ($h_{m,C}$) and the floating pan ($h_{m,p}$) against surface-to-air mixing ratio gradient (ΔX), a potential function of the type $h_m = c\ (\Delta X)^d$ fits well the data (R^2 = 0.94, Fig. 7).

$$h_m = 0.64(\Delta X)^{-0.64} \quad (13)$$

Fig. 7. Mass-transfer coefficient vs. surface-to-air mixing ratio gradient (weekly averages). Squares correspond to reservoir data and circles to class-A floating pan data

Adopting Eq. 13 for both water bodies, E_{hm} (mm day^{-1}) can be described by means of the following empirically derived potential function:

$$E_{hm} = 0.64(\Delta X)^{0.36} \quad (14)$$

This equation provides good evaporation estimates (weekly averages of daily values) for the covered reservoir (RMSE = 0.12, MBE = 0.08, MaxAE = 0.18mm day^{-1}) and the floating pan (RMSE = 0.09, MBE = 0.01, MaxAE = 0.16mm day^{-1}). It is worthwhile pointing out that, in spite of the large differences in size between the pan and the reservoir, a unique relationship (Eq. 14) can be used to derive *E* from the knowledge of a single explicative variable, the surface-to-air mixing ratio gradient.

Empirically derived mass-transfer equations can be used to predict the evaporation rate of a covered water surface, but local calibration is required. Eq. 14 is only suitable for analogous reservoirs covered with a material that have the same properties as the one tested in this study and under similar climatic conditions.

5. Summary and conclusions

A reservoir equipped with a black polyethylene suspended cover was fully monitored to register the evaporation rate and to characterise the microclimate conditions below the cover. A floating class-A pan was also deployed to assess if it could provide accurate evaporation measurements of the covered reservoir. The accuracy and adaptability of the energy budget, Penman and FAO-56 Penman-Monteith evaporation methods, commonly used for open-water surfaces has been tested for covered conditions. The mass-transfer formula based on the dimensionless Sherwood number to estimate evaporation under free and mixed convection conditions, which prevailed below the cover, has been described and tested. Besides, a simplified mass-transfer formula has been empirically derived to estimate evaporation in the covered reservoir from the knowledge of the surface-to-air mixing ratio gradient. The original findings derived from this study can be summarised as follows:

- A free convection regime was observed to prevail below the cover. Reliable and accurate weekly evaporation estimations under covered conditions can be obtained from formulae based on the dimensionless Sherwood number proposed for free convection conditions, which only require as input data the temperature and humidity of surrounding air and water surface temperature.

- The energy budget method and FAO-56 Penman-Monteith formula can also provide reasonably good evaporation estimations as long as the pertinent modifications are made in the calculation of the energy balance terms. However, these methods are not recommended for practical applications since they require more detailed input data than the Sherwood method and do not necessarily provide better accuracy.

- The estimations made with the Penman equation presented important overestimation due to the unsuitability for covered conditions of the wind function that is included in the formula to estimate the advective component.

- Whereas floating class-A pans have been reported to provide good estimations of open-water evaporation, our study highlights that they substantially overestimate covered reservoir evaporation. Although the water surface of the pan is under the same microclimate conditions as the reservoir surface, the peculiar characteristics of the tank affected substantially the surface temperature and hence evaporation rate. Using floating class-A pans to measure evaporation under covered reservoirs cannot be considered as an accurate and reliable means to determine water loss of covered water bodies.

- The analysis of the evaporation and mixing ratio data collected in two different water bodies demonstrated that a unique relationship can describe the tight dependence of the mass-transfer coefficient on the surface-to-air mixing ratio gradient, ΔX, for covered water reservoirs. Locally calibrated empirical relationships between E and ΔX, like the one presented in Eq. 14, can be a practical way to derive the weekly evaporation loss of covered reservoirs.

Acknowledgements

The authors acknowledge the Ministerio de Ciencia e Innovación (Spain) and FEDER (Fondo Europeo de Desarrollo Regional) for the financial support of this study through the grant AGL2010-15001.

Appendix

Formulae to compute Sh for free and mixed convection conditions

Assuming analogy between heat and mass transfer, Sh can be derived from the Nusselt number:

$$Sh = Nu\left(\frac{Sc}{Pr}\right)^{m} \tag{A.1}$$

where $Pr = \mu C_p/k$ is Prandtl number and $Sc = \nu/D$ is the Schmidt number, μ = viscosity (kg m^{-1} s^{-1}), C_p = specific heat at constant pressure (J kg^{-1} K^{-1}), ν = kinematic viscosity (m^2 s^{-1}) and the value of the exponent m = 1/3 for free and mixed convection conditions (Incropera and DeWitt, 1996; Jacobs and Verhoef, 1997; Pauken, 1999).

Nusselt number can be expressed as:

$$Nu = \frac{h_c \ L}{k} = cRa^n \tag{A.2}$$

where h_c (W m^{-2} K^{-1}) is the convective heat transfer coefficient, Ra is the Rayleigh number, c = 0.14 and n = 1/3 (Jacobs and Verhoef, 1997).

Ra is calculated from:

$$Ra = GrPr \tag{A.3}$$

where Gr is the Grashoff number:

$$Gr = \frac{\beta g L^3 (T_a - T_s)}{\nu^2} \tag{A.4}$$

where β = volumetric thermal expansion coefficient (K^{-1}) ($\beta = 1/T_a$ for perfect gases) and g is gravitational acceleration (m s^{-2}). To calculate Gr it is advisable to replace the difference $T_a - T_s$ by the difference of virtual temperature, T_{Va} - T_{Vs} (Monteith and Unsworth, 2008), to take into account the fact that moist air is less dense than dry air:

$$T_{Va} - T_{Vs} = (T_a - T_s) + 0.38(e_a T_a - e_s T_s)/P \tag{A.5}$$

where T_{Va} = virtual air temperature (K), T_{Vs} = virtual water surface temperature (K) and P = air pressure (kPa).

References

Ali, S., Ghosh, N.C., Singh, R., 2008. Evaluating best evaporation estimate model for water surface evaporation in semi-arid region, India. Hydrol. Process. 22, 1093-1106.

Allen, R.G., Pereira, L.S., Raes, D., Smith, M., 1998. Crop evapotranspiration. Guidelines for computing crop water requirements. Irrigation and Drainage Paper 56, FAO, Rome, pp. 300.

Bower, S.M., Saylor, J.R., 2009. A study of the Sherwood-Rayleigh relation for water undergoing natural convection-driven evaporation. Int. J. Heat Mass Tran. 52, 3055-3063.

Brutsaert, W., 1982. Evaporation into Atmosphere: Theory, History, and Applications. D. Reidel Publishing Company: Boston, MA.

Barnes, G.T., 2008. The potential for monolayers to reduce the evaporation of water from large water storages. Agr. Water Manage. 95, 339-353.

Carter, R., Kay, M., Weatherhead, K., 1999. Water losses in smallholder irrigation schemes. Agr. Water Manage. 40, 15-24.

Craig, I., Green, A., Scobie, M., Schmidt, E., 2005. Controlling Evaporation Loss from Water Storages. NCEA Publication No. 1000580/1: Queensland; 207.

Craig, I., 2006. Comparison of precise water depth measurements on agricultural storages with open water evaporation estimates. Agr. Water Manage. 85, 193-200.

Crawford, T.M., Duchon, C.E., 1998. An Improved Parameterization for Estimating Effective Atmospheric Emissivity for Use in Calculating Daytime Downwelling Longwave Radiation. J. Appl. Meteor. 38, 474-480.

Daigo, K., Phaovattana, V., 1999. Evaporation and percolation control in small farm ponds in Thailand. Jarq-jpn. Agr. Res. Q. 33, 47-56.

Delclaux ,F., Coudrain, A., Condom,T., 2007. Evaporation estimation on Lake Titicaca: a synthesis review and modelling. Hydrol. Process. 21, 1664-1677.

Foken, T., 2008. The energy balance closure problem: An overview. Ecol. Appl., 18, 1351-1367.

Fu, G., Liu, C., Chen, S., Hong, J., 2004. Investigating the conversion coefficients for free water surface evaporation of different evaporation pans. Hydrol. Process. 18, 2247-2262.

Gallego-Elvira, B., Baille, A., Martín-Gorriz, B., Maestre-Valero, J.F., Martínez-Alvarez, V., 2011. Energy balance and evaporation loss of an irrigation reservoir equipped with a suspended cover in a semiarid climate (south eastern Spain). Hydrol. Process. 25, 1694-1703.

Gianniou, S.K., Antonopoulos,V.Z., 2007. Evaporation and energy budget in lake Vegoritis, Greece. J. Hydrol. 345, 212-223.

Gokbulak, F., Ozhan, S., 2006. Water Loss Through Evaporation from Water Surfaces of Lakes and Reservoirs in Turkey. Official Publication of the European Water Association, EWA.

Hipsey, M.R., Sivapalan, M., 2003. Parameterizing the effect of a wind shelter on evaporation from small water bodies. Water Resour. Res. 39, 1339.

Incropera, F.P., DeWitt, D.P., 1996. Fundamentals of Heat and Mass Transfer., fourth ed. John Wiley & Sons, New York.

Jacobs, A.F.G., Verhoef, A., 1997. Soil evaporation from sparse natural vegetation estimated from Sherwood numbers. J. Hydrol. 189, 443-452.

Martínez-Alvarez,V., Gonzalez-Real, M.M., Baille, A., Molina-Martínez, J.M., 2007. A novel approach for estimating the pan coefficient of irrigation water reservoirs. Application to South Eastern Spain. Agr. Water Manag. 92, 29-40.

Martínez-Alvarez,V., Gonzalez-Real, M.M., Baille, A., Maestre-Valero, J.F., Gallego-Elvira, B., 2008. Regional assessment of evaporation from agricultural irrigation reservoirs in a semiarid climate. Agr. Water Manage. 95, 1056-1066.

Martínez-Alvarez,V., Maestre-Valero, J.F. , Martín-Górriz, B., Gallego-Elvira, B., 2010. Experimental assessment of shade-cloth covers on agricultural reservoirs for irrigation in south-eastern Spain. Span. J. Agric. Res. S2, 122-133.

Masoner, J.R., Stannard, D.I., Christenson, S.C., 2008. Differences in evaporation between a floating pan and class a pan on land. J. Am. Water Resour. As. 44, 552-561.

Monteith, J.L., Unsworth, M.H., 2008. Principles of Environmental Physics, third ed. Elsevier Inc., Oxford.

Mugabe, F.T., Hodnett, M.G., Senzanje, A., 2003. Opportunities for increasing productive water use from dam water: a case study from semi-arid Zimbabwe. Agr. Water Manage. 62, 149-163.

Pauken, M.T., 1998. An experimental investigation of combined turbulent free and forced evaporation. Exp. Therm. Fluid. Sci., 18, 334-340.

Penman, H.L., 1948. Natural Evaporation from Open Water, Bare Soil and Grass. Proceedings of the Royal Society of London Series A-Mathematical and Physical Sciences, 193: 120.

Rosenberry, D.O., Winter, T.C., Buso, D.C., Likens, G.E., 2007. Comparison of 15 evaporation methods applied to a small mountain lake in the northeastern USA. J. Hydrol. 340, 149-166.

Singh, V.P., Xu, C.Y., 1997. Evaluation and generalization of 13 mass-transfer equations for determining free water evaporation. Hydrol. Process. 11, 311-32.

Valiantzas, J.D., 2006. Simplified versions for the Penman evaporation equation using routine weather data. J. Hydrol. 331, 690-702.

Xu, C.Y., Singh, V.P., 2000. Evaluation and generalization of radiation-based methods for calculating evaporation. Hydrol. Process. 14, 339-349.

Xu, C.Y., Singh, V.P., 2001. Evaluation and generalization of temperature-based methods for calculating evaporation. Hydrol. Process. 15, 305-319.

Table1
Click here to download Table: Table1.docx

Table 1. Reference weekly evaporation reduction factors achieved by the cover during the 11-week experimental period

Week	*E* (mm day^{-1})	ET_o (mm day^{-1})	*RF* (%)
1	0.75	5.55	0.86
2	0.92	5.72	0.84
3	0.82	5.77	0.86
4	0.68	5.68	0.88
5	0.67	5.89	0.89
6	0.91	5.75	0.84
7	0.66	5.32	0.88
8	0.60	5.22	0.88
9	0.78	5.41	0.86
10	0.78	5.44	0.86
11	0.76	5.20	0.85
Average	0.76	5.54	0.86
SD	0.10	0.24	0.02

Table 2. Values of Ra, Re^2 and Ra/Re^2 to determine the type of convection

	Reservoir			Class A pan		
	Ra	Re^2	Ra/Re^2	*Ra*	Re^2	Ra/Re^2
Mean	$4.56 \cdot 10^{13}$	$0.43 \cdot 10^{12}$	115	$3.81 \cdot 10^{8}$	$2.39 \cdot 10^{8}$	1.35
SD	$8.05 \cdot 10^{12}$	$0.10 \cdot 10^{12}$	36	$1.24 \cdot 10^{8}$	$2.90 \cdot 10^{8}$	0.56
Max	$6.35 \cdot 10^{13}$	$0.75 \cdot 10^{12}$	226	$7.03 \cdot 10^{8}$	$3.07 \cdot 10^{8}$	2.45
Min	$1.38 \cdot 10^{13}$	$0.24 \cdot 10^{12}$	28	$1.85 \cdot 10^{8}$	$2.86 \cdot 10^{8}$	0.55

Table3
Click here to download Table: Table3_R3.HYDROL11970.doc

Table 3. Mean values and Standard Deviation of weekly averages of daily evaporation measurements and estimations for the 11-week experimental period. Statistical estimators for estimations of covered reservoir evaporation

	Measurements		Estimations			
	Covered reservoir	Floating pan	Sherwood	Energy Budget	Penman	PM-FAO56
mm day^{-1}	E	E_{pan}	E_{Sh}	E_{EB}	E_P	E_{PM}
MEAN	0.76	1.19	0.74	1.00	1.81	0.91
SD	0.10	0.08	0.13	0.11	0.11	0.09
RMSE	-	0.47	0.08	0.30	1.11	0.22
MBE	-	0.44	-0.01	0.24	1.05	0.14
MaxAE	-	0.61	0.18	0.58	1.28	0.46

Figure1

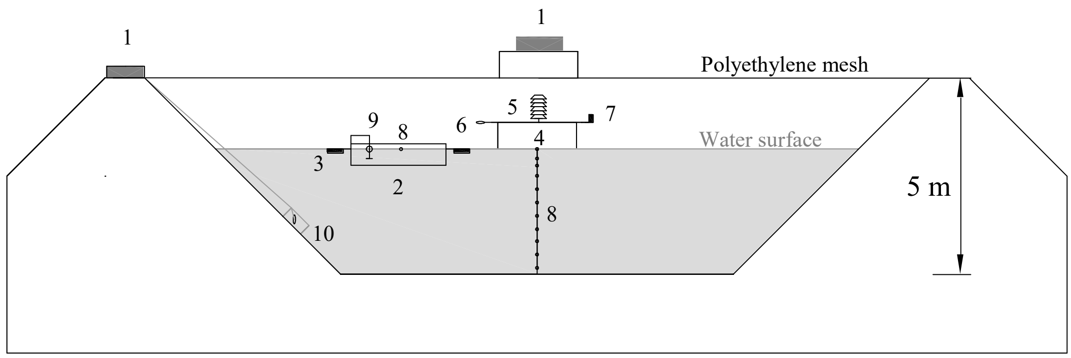

1 Dataloggers; 2 Floating class-A pan; 3 Pan floats; 4 Raft; 5Air temperature and relative humidity probe; 6 Low-wind sensor ; 7 Infrared temperature sensor; 8 Water temperature probes; 9 Water level sensor; 10 Pressure transducer.

Figure 1. Data collection layout in the covered reservoir (the vertical scale is exaggerated for clarity)

Figure2

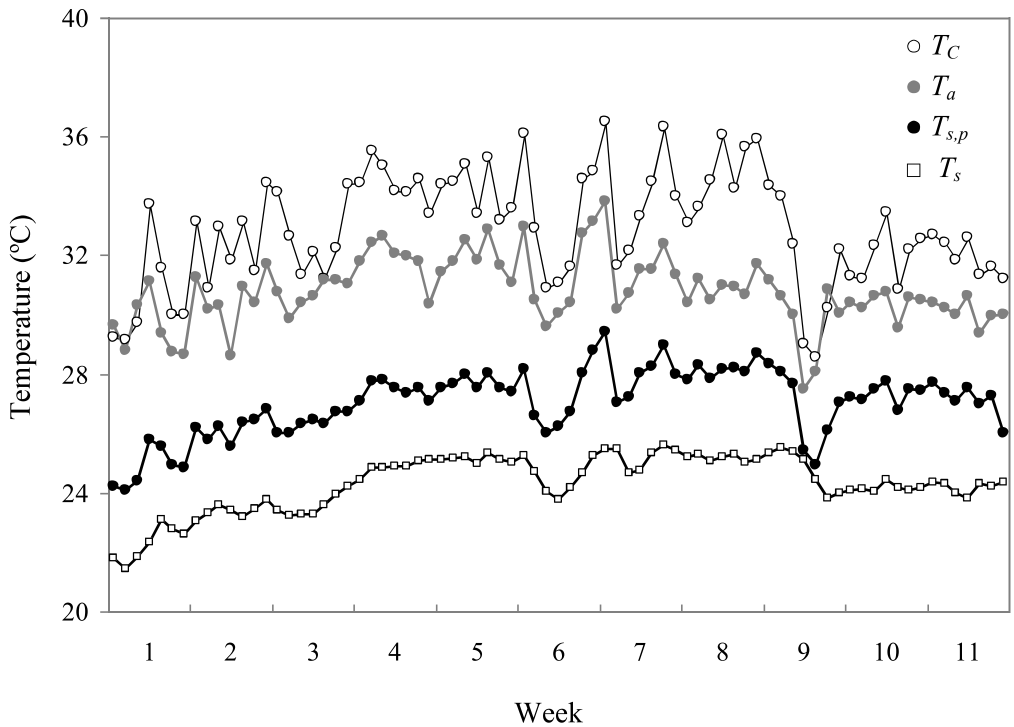

Figure 2. Daily evolution of temperature of the cover (T_C), inner air (T_a) and water surface of the floating pan ($T_{s,p}$) and of the reservoir (T_s), during the 11-week experimental period

Figure3

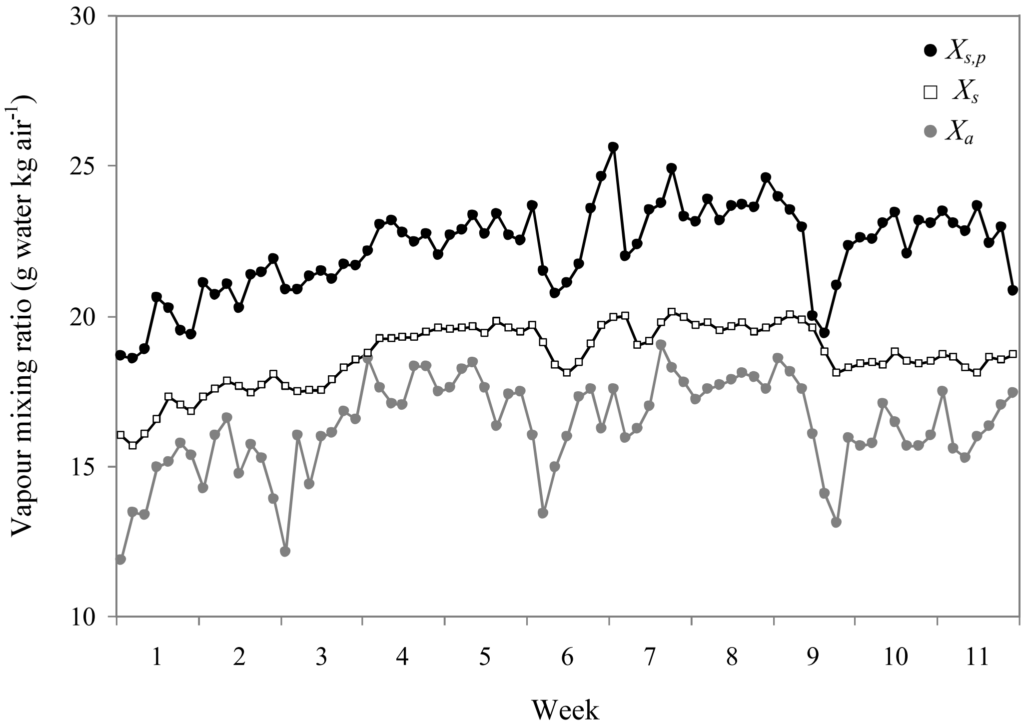

Figure 3. Daily evolution of water vapour mixing ratio of the floating class-A pan ($X_{s,p}$), of the reservoir (X_s) and of the inner air (X_a), during the 11-week experimental period

Figure4

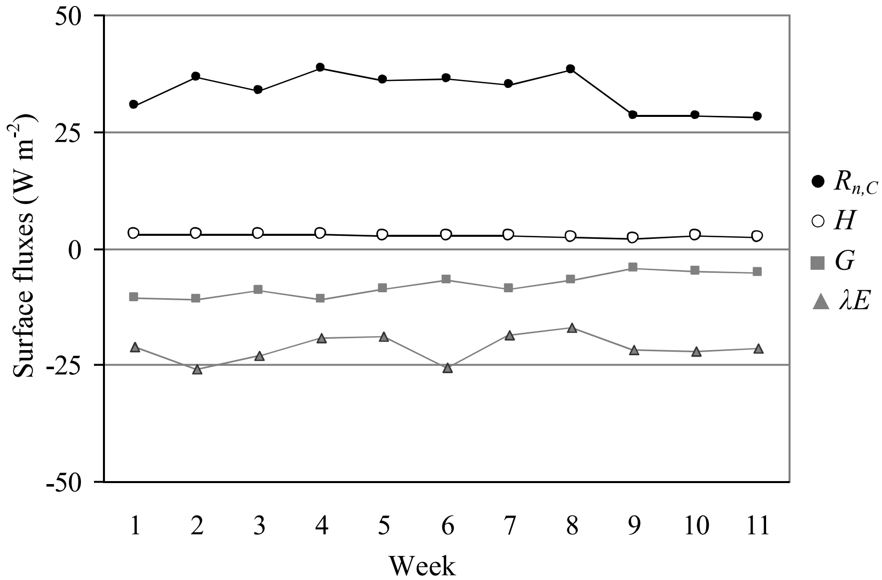

Figure 4. Weekly evolution of the energy fluxes at the covered water surface. Experimental period: 12th June to 27th August 2009.

Figure5

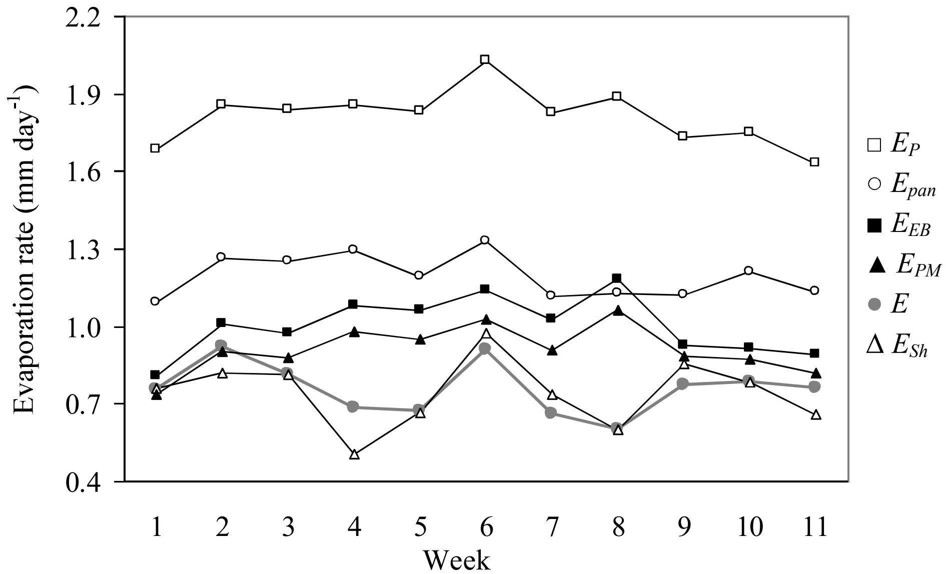

Figure 5. Comparison of weekly averages of daily values of measurements of covered reservoir evaporation (E) with floating class-A pan measurements (E_{pan}) and estimations calculated by Sherwood (E_{Sh}), Energy Budget (E_{EB}), Penman (E_P) and PM-FAO56 (E_{PM}) methods. Experimental period: 12th June to 27th August 2009.

.

Figure6

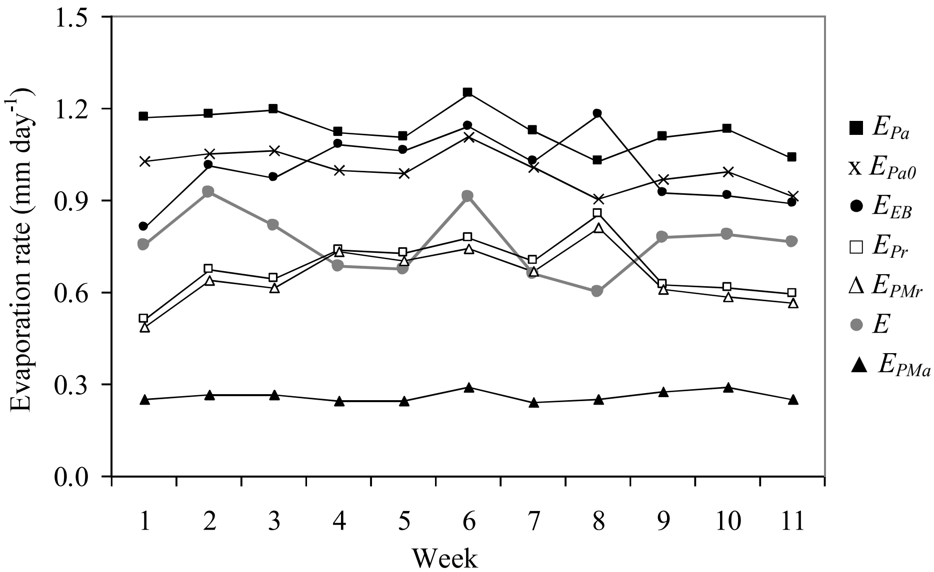

Figure 6. Evolution of weekly averages of daily values of: the radiative and advective terms of the combination methods (Penman (E_P) and PM-FAO56 (E_{PM})), measurements of covered reservoir evaporation (E) and estimations calculated by the Energy Budget method (E_{EB}). The subindex "a" refers to advective, "r" to radiative, and "0" indicates that wind speed was set to zero for calculations. Experimental period: 12th June to 27th August 2009.

.

Figure7

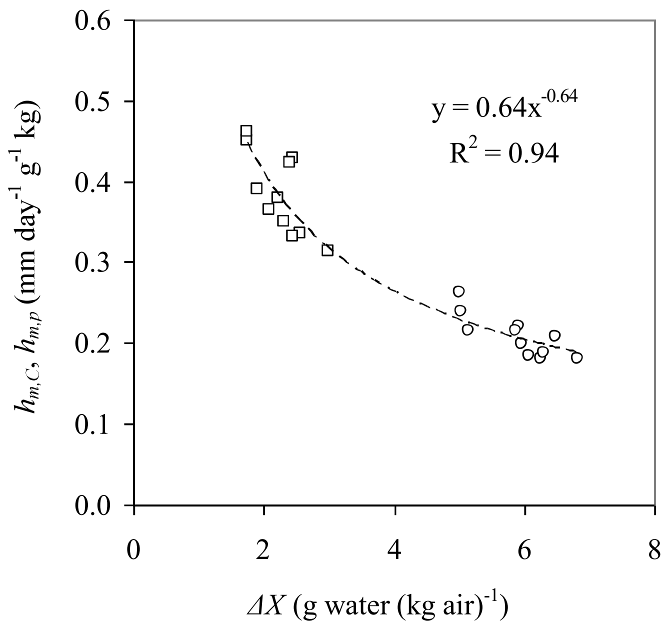

Figure 7. Mass transfer coefficient vs. surface-to-air mixing ratio gradient (weekly averages). Squares correspond to reservoir data and circles to class-A floating pan data